

## Article

# Charging Scheduling of Electric Vehicles Considering Uncertain Arrival Times and Time-of-Use Price

Zhaojie Wang<sup>1,2,\*</sup>, Feifeng Zheng<sup>3</sup> and Ming Liu<sup>4</sup> <sup>1</sup> Business School, Ningbo University, Ningbo 315211, China<sup>2</sup> Merchants' Guild Economics and Cultural Intelligent Computing Laboratory, Ningbo University, Ningbo 315211, China<sup>3</sup> Glorious Sun School of Business and Management, Donghua University, Shanghai 200051, China; ffzheng@dhu.edu.cn<sup>4</sup> School of Economics and Management, Tongji University, Shanghai 200092, China; mingliu@tongji.edu.cn

\* Correspondence: wangzhaojie1@nbu.edu.cn

**Abstract:** To advance sustainable transportation solutions, this work investigates an electric vehicle charging scheduling problem under the uncertainty of vehicle arrival times. Given a set of appointed electric vehicles, the objective of the considered problem is to explore charging strategies that minimize the total charging cost for the charging station. To address this problem, this work first establishes a mixed-integer programming model. Then, an enhanced sample average approximation approach alongside two versions of distribution-free approaches are applied to solve the studied problem. Additionally, this study introduces a BP neural network-enhanced distribution-free approach to efficiently resolve the problem. Finally, numerical experiments are conducted to demonstrate the effectiveness of the proposed approaches.

**Keywords:** charging scheduling; electric vehicles; uncertain arrival times; distribution-free; numerical experiments



Academic Editors: Jack Barkenbus, Giovanni Leonardi and Nicoletta Matera

Received: 28 October 2024

Revised: 20 December 2024

Accepted: 27 January 2025

Published: 29 January 2025

**Citation:** Wang, Z.; Zheng, F.; Liu, M. Charging Scheduling of Electric Vehicles Considering Uncertain Arrival Times and Time-of-Use Price. *Sustainability* **2025**, *17*, 1100. <https://doi.org/10.3390/su17031100>

**Copyright:** © 2025 by the authors. Licensee MDPI, Basel, Switzerland. This article is an open access article distributed under the terms and conditions of the Creative Commons Attribution (CC BY) license (<https://creativecommons.org/licenses/by/4.0/>).

## 1. Introduction

With the increasing popularity of electric vehicles (EVs) due to their environmentally friendly advantages, the demand for EV charging services is growing rapidly [1–7]. However, in scheduling practices, charging stations prioritize serving their affiliated bus companies by providing recharging services for electric buses (EBs). To enhance the efficiency of charging infrastructure and maximize revenue generation, idle periods of EV chargers are utilized by charging stations to accommodate pre-booked electric vehicles. Consequently, EV chargers might not always be available throughout the entire decision-making process. The limited number of available EV chargers poses challenges for decision-makers in making efficient scheduling decisions for EV charging [8,9].

The scheduling of EV charging encounters challenges that arise from various uncertainties [5]. To facilitate advanced scheduling, the charging station requires EV users to input their estimated arrival times, required charging levels, and other relevant details into the reservation system for completing the booking process, as depicted in Figure 1. Due to uncertain factors such as road conditions and driver's driving skills, EVs are usually with uncertain EV arrival times. In practice, decision-makers at charging stations may learn some characters or approximate distributions of uncertain EV arrival times. However, in most situations, historical data only provide upper and lower information other than accurate specific distribution. This uncertainty causes the deviation in the execution of

charging plans, especially the delay of some charging activities. To enhance customer satisfaction, it is essential to manage the likelihood of delayed charging within an acceptable risk threshold.

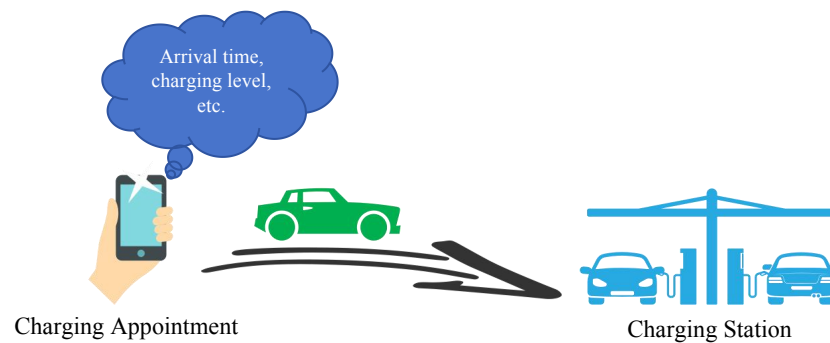


**Figure 1.** Illustration of the research background.

As illustrated in Figure 2, the implementation of time-of-use (TOU) pricing could significantly impact supply-side management strategies. These strategies focus on reducing costs of charging services and optimizing load distribution at charging stations during various time periods [10]. Moreover, decision-makers encounter the challenge of striking a delicate balance between the costs associated with electricity demand and the risk level incurred due to delayed charging. This necessitates the careful consideration of this trade-off in order to minimize the overall expenses associated with the charging process. As a result, decision-makers face an additional challenge in making scheduling decisions.

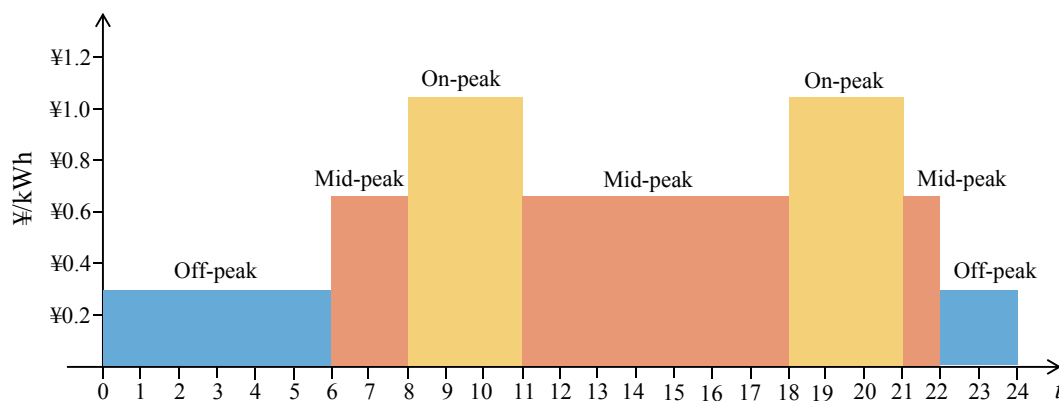


**Figure 2.** Time-of-use tariffs during each day in Shanghai city (except July to September).

While some existing studies have formulated the charging function of electric vehicles as a linear model, empirical evidence from charging practices suggests that the relationship between state of charge (SoC) and charging duration is nonlinear [11–14]. It is evident that an appropriate characterization of the charging function plays a crucial role in enabling decision-makers to accurately assess the necessary charging duration for electric vehicles. Therefore, it is imperative to establish a reasonable charging function to facilitate informed decision-making regarding charging scheduling.

Numerous studies have addressed EV charging scheduling through optimization-based frameworks, including deterministic approaches, stochastic programming, and robust optimization. Deterministic models often struggle to capture uncertainties in EV arrivals, charging demands, and grid conditions, leading to suboptimal scheduling outcomes in dynamic real-world scenarios. Stochastic programming approaches, while capable of handling uncertainties, typically rely on full distributional knowledge, which may not always be available or accurate. On the other hand, robust optimization techniques provide

solutions that are overly conservative, potentially leading to higher costs or inefficiencies. These limitations highlight the need for methods that balance robustness, flexibility, and computational efficiency in EV charging scheduling.

To address the considered problem, this work investigates a charging scheduling of electric vehicles considering uncertain EV arrival times. Our objective is to determine a schedule that minimizes total charging costs in an environment with uncertainty and time-of-use mechanisms. Similar to [11,14], this work employs a piecewise linear approximation to capture the nonlinear nature of the charging process. The contributions of our research are summarized as follows:

1. In line with charging practices, the EV charging scheduling problem considering uncertain EV arrival times, the TOU mechanism, and the nonlinear charging function is first introduced in this work;
2. For addressing this problem, a K-means enhanced SAA (Sample Average Approximation) approach and distribution-free approaches are, respectively, established by this work;
3. To the best of our knowledge, the BP neural network is applied for the first time to enhance the distribution-free approach for addressing the EV charging scheduling problem. Numerical experiments are conducted to demonstrate the effectiveness of our approaches.

The remainder of this paper is organized as follows. Section 2 provides a brief literature review. Section 3 gives a brief description of the studied problem and establishes a stochastic mixed-integer programming model. Section 4 establishes SAA models and distribution-free models. Section 5 conducts numerical experiments to demonstrate the effectiveness of the proposed approaches. Section 6 concludes this work.

## 2. Literature Review

The EV scheduling problem has been well investigated in the literature [15–17]. Below, we give a brief view of five key areas of related studies, i.e., the optimization of charging costs, mitigation of power grid constraints, reduction in EV waiting time, and management of charging station capacity.

### 2.1. Optimization of Charging Costs

Previous studies have primarily focused on minimizing objectives related to charging costs. Sassi and Oulamara (2017) addressed the optimization of vehicle assignment to tours and charging costs in an electric vehicle scheduling problem. They proposed a mixed-integer linear programming formulation for modeling this problem, followed by the introduction of two heuristics to handle large instances effectively [18]. Expanding on the theme of cost minimization, Koufakis et al. (2020) tackled the single charging station electric vehicle charging problem by developing a mixed-integer programming model that aims to minimize total charging costs. Additionally, they presented both offline and online scheduling algorithms for efficient charging at a single station [19]. To resolve conflicts at charging stations, Kakkar et al. (2022) introduce a blockchain and Internet of Things-based consensus mechanism for secure and trustworthy electric vehicle scheduling at these locations [20]. Cao et al. (2023) considered a joint routing and wireless charging scheduling problem with microwave power transfer systems in mind, aiming to minimize travel distance, charging costs, and battery degradation when IoEVs provide shuttle services. They propose a customized benders decomposition algorithm called “routing and charging customized benders decomposition” (RCBD), along with an improved version called the IRCBD algorithm to enhance time efficiency based on extensive simulation results, demonstrating the effectiveness and correctness of their proposed scheduling algorithms [21]. Wang and Wu

(2024) explored the optimization of real-time charging schedules for large-scale EV parking lots, introducing a semi-decentralized scheduling framework that balances scalability and economic efficiency. The study employs a chance-constrained model with a Gaussian mixture model to estimate aggregate charging needs while addressing demand uncertainties, followed by the allocation of charging energy references to individual chargers. Simulation results highlight that this approach significantly improves scheduling efficiency at a marginal cost of revenue, providing a promising alternative to fully centralized or decentralized schemes [22].

Reinforcement learning (RL) methods have been employed in several studies to address EV charging scheduling problems. Park and Moon (2022) proposed a multi-agent deep reinforcement learning approach to minimize the operating cost of electric vehicles, demonstrating its effectiveness through numerical experiments [2]. Hossain et al. (2023) introduced a genetic algorithm-based reinforcement learning framework for studying EV charging scheduling, showcasing accelerated convergence and significantly enhanced cost-friendly privacy with their proposed framework [23].

## 2.2. Mitigation of Power Grid Constraints

Several studies are focused on addressing constraints associated with the power grid. Wang et al. (2023) investigated the EV charging scheduling problem by considering uncertain EV departures, aiming to support load flattening at the distribution level of the utility grid. Meanwhile, a holistic methodology is proposed by them to formulate and mitigate the impact of unexpected trip uncertainty [24]. Nimalsiri et al. (2022) introduced two decentralized schemes for scheduling EV charges in residential communities connected to the electric grid, with the objective of shaping the load curve [25]. Frendo et al. (2021) presented an open-source package that incorporates a smart charging algorithm, effectively addressing EV charging scheduling problems, as demonstrated by experimental results [26]. Zhao et al. (2024) investigated the problem of electric vehicle charging scheduling with the objective of flattening aggregate load on the power grid and reducing peak demand. For solving this problem, a two-level hierarchical charging scheduling method is first proposed by them, and then a comprehensive set of experiments is carried out to examine the effectiveness of the developed two-level scheduling scheme [27]. Aljohani et al. (2024) studied the challenges of managing large-scale electric vehicle (EV) integration by proposing a two-layer optimization framework based on the Stackelberg leader–follower game to coordinate EV charging. The framework models practical economic, technical, and operational variables and solves the optimization problem using mixed-integer quadratic programming (MIQP). The results show that the proposed strategy effectively influences EV charging via dynamic energy price signals and achieves optimal energy exchange, reducing overall system costs [28]. Jia et al. (2023) examined the impact of uncertain EV charging and discharging behavior on the stability of distribution networks, highlighting the sensitivity of EV loads to electricity pricing. For solving the problem, they proposed a virtual power plant optimization scheduling model that leverages incentive-based demand response strategies and dynamic load compensation under time-of-use pricing. The method proposed by them, validated using real-world data from an EV charging station in Zhengzhou, demonstrates its effectiveness in improving grid stability and economic performance [29].

## 2.3. Reduction in Electric Vehicle Waiting Time

Several studies focus on reducing the waiting time for EVs. Tan et al. (2023) formulated a bi-objective charging and discharging scheduling problem, aiming to balance the trade-off between time-aware fairness and the overall waiting time of EVs, with a primary objective of

minimizing individual waiting times. They proposed an online scheduling algorithm based on dynamic schedulable time, and their experimental results demonstrate that their method effectively reduces total waiting time [30]. Similarly, Arikumar et al. (2024) introduced a software-defined network-assisted EV charge scheduling and management strategy designed to optimize charge scheduling and provide personalized charging services. Their experimental analysis reveals that this method is significantly more efficient compared to existing algorithms [31].

#### 2.4. Management of Charging Station Capacity

Constraints related to the capacity of charging stations have been considered in numerous existing studies. de Vos et al. (2024) addressed the EV scheduling problem by taking into account the limited capacity of charging stations. To tackle this issue, they extended a connection-based network and developed a model for recharging actions. Subsequently, they formulated the electric vehicle scheduling problem as a path-based binary program and employed two heuristics to find integer-feasible solutions [32]. With regard to the limited number of charging piles and maximum instantaneous power at charging stations, Wu et al. (2023) proposed an EV charging scheduling strategy to handle the EV charging scheduling problem under a time-of-use price mechanism [9]. To address insufficiencies in charging capacity caused by mismatches between charging stations and EV charging loads, Chen et al. (2022) proposed a hierarchical scheduling model for EVs that aimed to achieve optimal matching between different charging facilities and EVs [33]. Shahmoradi et al. (2022) presented an efficient method for solving the electric vehicle charging scheduling problem (EVCSP), which was inspired by an actual charging station scenario. The primary constraint in this problem lies in balancing power consumption among multiple lines, resulting in limitations on simultaneous device chargeability [4]. Diefenbach et al. (2023) introduced a novel electric vehicle scheduling problem with multiple charging stations in an in-plant logistics setting with the objective of minimizing the required fleet size. To solve this problem, they presented an integer programming model and an exact branch-and-check solution procedure [34]. Zhou et al. (2024) investigated a time-dependent electric vehicle routing and scheduling problem with time windows (TDEVRSPW) to address energy capacity limitations and high consumption in EVs. A mixed-integer linear programming (MILP) model was developed to optimize small-scale problems, while a variable neighborhood search with a partial model method was proposed for large-scale scenarios. Numerical experiments show significant energy savings and strong performance [35].

Based on the above observations and Table 1, it can be inferred that current research mainly focuses on deterministic charging scheduling problems, with limited consideration of uncertainty in practice. Nonlinear charging functions are rarely taken into account, and few studies have addressed the issue of EV charger availability over the decision-making horizon. Most existing studies rely on heuristic methods to quickly respond to EV charging scheduling problems. Motivated by these findings, we propose an EV charging scheduling problem that considers uncertain EV arrival times and nonlinear charging functions. To solve this problem, we developed a K-means enhanced SAA approach and distribution-free approaches. Numerical experiments demonstrate the effectiveness of the proposed approach.

**Table 1.** Related studies of the EV charging scheduling problem.

Study	Nonlinear Charging Function	Uncertain Arrival Times	TOU	EV Charger Unavailability	Solution Method
Ref. [18]			✓		MILP, Heuristics
Ref. [19]					MILP, OFA, ONA
Ref. [20]					Heuristic
Ref. [21]			✓		RCBD
Ref. [22]		✓	✓		SDRCSS
Ref. [24]				✓	ADMM
Ref. [25]					MILP, C-VF, C-VF-PS
Ref. [26]			✓		Heuristic
Ref. [28]			✓		MIQP
Ref. [29]			✓		MILP
Ref. [30]			✓		ONA
Ref. [31]					SEVC
Ref. [32]					CG, Heuristic
Ref. [9]			✓		AGA
Ref. [33]					QPSA
Ref. [4]					EDA
Ref. [34]	✓				B&C
Ref. [2]	✓		✓		RL
Ref. [23]	✓		✓		RL, GA
Ref. [27]	✓		✓		RL, MDP
Ref. [35]			✓		VNS-PM
this work	✓	✓	✓	✓	MILP, DFA

Note: MILP: mixed-integer linear programming; OFA: offline algorithm; ONA: online algorithm; RCBD: routing and charging customized benders decomposition; SDRCSS: semi-decentralized real-time charging scheduling scheme; ADMM: alternating direction method of multipliers; C-VF: coordinated valley-filling; C-VF-PS: coordinated valley-filling and peak-shaving; MIQP: mixed-integer quadratic programming; SEVC: software-defined network-assisted EV charge; CG: column generation; AGA: adaptive genetic algorithm; QPSA: quantum particle swarm algorithm; EDA: estimation of distribution algorithm; B&C: branch-and-check; RL: reinforcement learning; MDP: Markov decision process; VNS-PM: variable neighborhood search with partial model; DFA: Distribution-Free Approaches

### 3. Problem Description

Consider a charging station that is equipped with a set of available EV chargers  $\mathcal{M} = \{1, 2, \dots, |\mathcal{M}|\}$  (refer to Figure 3). The station has received a collection of appointed charging demands  $\mathcal{N} = \{1, 2, \dots, |\mathcal{N}|\}$ , where each demand corresponds to some EVs and planned state-of-charging (SoC) amount. Notice that we simplify SoC as the charging level for ease of model construction and solution. Specifically, we define the charging level as a discrete representation of SoC, where a charging level of 1 corresponds to 1% SoC, and a charging level of 100 corresponds to 100% SoC. This discrete approach enables efficient problem formulation and solution while ensuring sufficient accuracy for practical applications. Influenced by road conditions, driver proficiency, etc., the arrival time of each EV typically exhibits characteristics of uncertainty. Such an uncertainty of EV arrival times leads to unpredictability in the start charging time and charging duration of each EVs. Additionally, reflecting real-world charging practices, we consider that the cost of electricity demand varies over time, i.e., TOU. Under limitations of the TOU pricing, decision-makers are required to robustly determine the start and end charging times for any EV. Due to the occurrence of uncertain EV arrival times, formulating such decisions presents significant

challenges. In this work, we aim to develop a feasible solution that minimizes the total charging cost as effectively as possible.

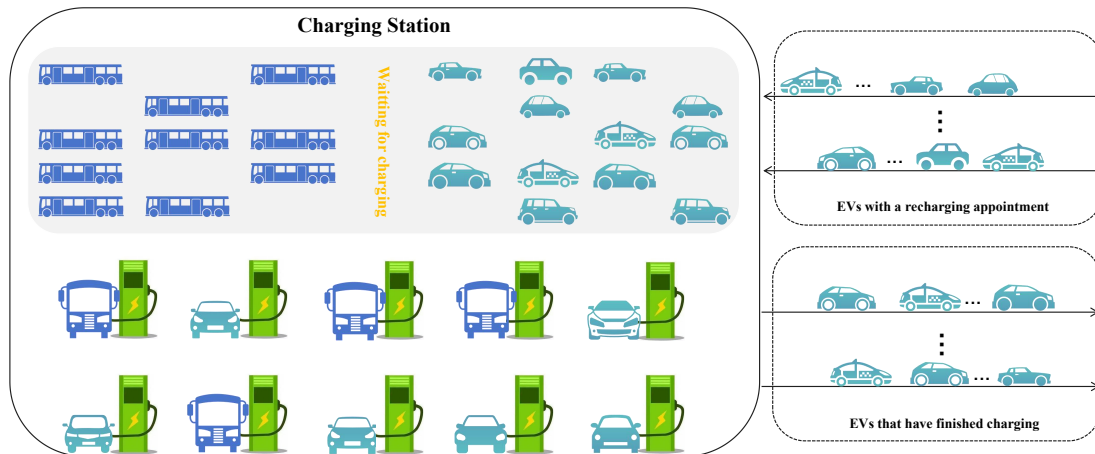


**Figure 3.** Illustration of a charging station.

Before solving this problem, we introduce four fundamental assumptions as follows:

1. In line with effective charging protocols, the charging duration of any EV is continuous, and preemption is not allowed;
2. In this work, continuous charging of EVs fails to account for the time needed to switch between charging stations during the charging process;
3. Each EV charger is designed to maintain a constant power output;
4. The time horizon covers three types of electricity prices, i.e., peak price, off-peak price, and valley price.

### 3.1. Mathematical Model

Below, we first introduce parameters and decision variables associated with the considered problem, and then present the established mathematical model.

#### 3.1.1. Input Parameters

$\mathcal{M}$ : Set of EV chargers, indexed by  $i$ , i.e.,  $i \in \mathcal{M} = \{1, 2, \dots, |\mathcal{M}|\}$ ;

$\mathcal{N}$ : Set of appointed EVs, indexed by  $j$ , i.e.,  $j \in \mathcal{N} = \{1, 2, \dots, |\mathcal{N}|\}$ ;

$\mathcal{T}$ : Set of time points, indexed by  $t$ , i.e.,  $t \in \mathcal{T} = \{1, 2, \dots, |\mathcal{T}|\}$ ;

$r_j$ : Uncertain arrival time of EV  $j \in \mathcal{N}$ ;

$idle_{it}$ : A binary parameter, equal to 1 indicates that EV charger  $i \in \mathcal{M}$  is available at time  $t \in \mathcal{T}$ , 0 otherwise;

$a_j$ : Initial SoC of EV  $j \in \mathcal{N}$ ;

$l_j$ : Charging level of EV  $j \in \mathcal{N}$ ;

$p_j$ : Charging duration time of EV  $j \in \mathcal{N}$ ;

$v_1$ : Charging speed ( $kW$ ) associated with less than or equal to 80 SoC;

$v_2$ : Charging speed ( $kW$ ) associated with large than 80 SoC;

$c_t^e$ : Electricity price at time  $t \in \mathcal{T}$ ;

$P$ : Power of each EV charger  $i \in \mathcal{M}$  (in  $kW \cdot h$ );

$w_{\max}$ : Given maximum waiting time for each EV;

$\varepsilon$ : Given risk level;

$\Delta t$ : Discrete time interval (in minutes);

$M$ : A sufficiently large positive integer.

### 3.1.2. Decision Variables

$x_{jt}$ : A binary variable, when equal to 1 indicates that EV  $j \in \mathcal{N}$  is charged at time  $t \in \mathcal{T}$ , 0 otherwise;

$z_{jt}$ : A binary variable, when equal to 1 indicates that start charging time of EV  $j \in \mathcal{N}$  is time point  $t \in \mathcal{T}$ , 0 otherwise;

$s_j$ : Start charging time of EV  $j \in \mathcal{N}$ .

The objective function is formulated to minimize the total charging cost.

$$[\mathbf{P1}] \min \sum_{j \in \mathcal{N}} \sum_{t \in \mathcal{T}} x_{jt} \cdot c_t^e \cdot \frac{P}{60} \cdot \Delta t \quad (1)$$

subject to

$$\sum_{t \in \mathcal{T}} z_{jt} = 1, \quad \forall j \in \mathcal{N} \quad (2)$$

$$\sum_{j \in \mathcal{N}} x_{jt} \leq \sum_{i \in \mathcal{M}} \text{idle}_{it}, \quad \forall t \in \mathcal{T} \quad (3)$$

$$x_{jt} \geq z_{jt}, \quad \forall j \in \mathcal{N}, t \in \mathcal{T} \quad (4)$$

$$s_j = \sum_{t \in \mathcal{T}} t \cdot z_{jt}, \quad \forall j \in \mathcal{N} \quad (5)$$

$$s_j \geq r_j, \quad \forall j \in \mathcal{N} \quad (6)$$

$$x_{jt'} \geq 1 - M \cdot (1 - z_{jt}), \quad \forall j \in \mathcal{N}, t \in \mathcal{T}, t' \in [t, t + [p_j]] \quad (7)$$

$$\mathcal{P}\{s_j \leq r_j + w_{\max}\} \geq 1 - \epsilon, \quad \forall j \in \mathcal{N} \quad (8)$$

$$x_{jt}, z_{jt} \in \{0, 1\}, \quad \forall j \in \mathcal{N}, t \in \mathcal{T} \quad (9)$$

$$s_j \in \mathbb{R}^+, \quad \forall j \in \mathcal{N} \quad (10)$$

Constraint (2) ensures that each EV  $j \in \mathcal{N}$  is charged throughout the entire time horizon. Constraint (3) guarantees that the number of EVs charged at any time  $t \in \mathcal{T}$  is not larger than that of given EV chargers. Constraints (4)–(6) calculate the start charging time of EV  $j \in \mathcal{N}$ . Constraint (7) ensures that the charging duration of EV  $j \in \mathcal{N}$  is continuous and uninterrupted. Chance Constraint (8) incorporates the uncertainty of EV arrival times through a chance constraint  $P(s_j \leq r_j + w_{\max}) \geq 1 - \epsilon$ . This constraint ensures that the start charging time  $s_j$  cannot exceed the arrival time  $r_j$  plus the maximum allowable waiting time  $w_{\max}$  with a probability of at least  $1 - \epsilon$ . By introducing this constraint, the model accounts for the randomness in EV arrival times, ensuring robust scheduling decisions under uncertainty. Notice that the symbol  $\mathcal{P}\{\bullet\}$  denotes the probability associated with the occurrence of event  $\bullet$ . Constraints (9)–(10) give the range of variables, where  $\mathbb{R}^+$  represents the set of real numbers.

The proposed model is formulated as a mixed-integer programming (MIP) problem, which is known to be NP-hard. As such, the computational complexity of the model increases exponentially with the number of decision variables and constraints. The key factors influencing this growth include the number of EVs, the number of time slots, and the number of scenarios generated for uncertainty modeling. While MIP problems are computationally challenging, advances in modern solvers allow us to solve practical problem sizes efficiently, as demonstrated in Section 4.

### 3.2. Nonlinear Charging Function

Below is a piecewise equation associated with charging level and initial SoC.

$$p_j = \begin{cases} (l_j - a_j)/v_1, & l_j < 80\%SoC \\ \max\{80 - a_j, 0\}/v_1 + (l_j - 80)/v_2, & l_j \geq 80\%SoC \end{cases}, \quad \forall j \in \mathcal{N} \quad (11)$$

As shown in Figure 4, under reasonable assumptions (see [11,14,36]), i.e., the initial SoC satisfying  $a_j \leq 80$ , the piecewise equation (11) can be rewritten as follows:

$$p_j = \begin{cases} (l_j - a_j)/v_1, & l_j < 80\%SoC \\ (80 - a_j)/v_1 + (l_j - 80)/v_2, & l_j \geq 80\%SoC \end{cases}, \quad \forall j \in \mathcal{N} \quad (12)$$

Below, we first introduce a binary auxiliary parameter  $y_j$  to function (12), and then simplify this charging time function:

$y_j$ : A binary auxiliary parameter, equal to 1 indicates that  $l_j \geq 80$ , 0 otherwise.

$$\begin{aligned} p_j &= ((l_j - a_j)/v_1) \cdot (1 - y_j) + ((80 - a_j)/v_1 + (l_j - 80)/v_2) \cdot y_j \\ &= l_j \cdot (1 - y_j)/v_1 + y_j \cdot 80/v_1 + y_j \cdot (l_j - 80)/v_2 - a_j/v_1, \quad \forall j \in \mathcal{N} \end{aligned}$$

With the support of such a binary auxiliary parameter  $y_j$ ,  $p_j$  is a linear function of  $l_j$ .

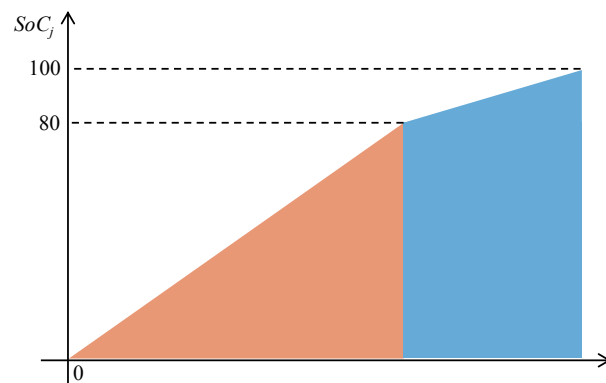


Figure 4. Illustration of a charging function.

## 4. Solution Approaches

Based on the known degree of distribution information of uncertain variable  $r_j$  ( $j \in \mathcal{N}$ ), we apply the K-means enhanced SAA, denoted as the KSAA approach, and the distribution-free approaches to solve the studied problem. Specifically, the KSAA approach can be employed to address the studied problem when precise distribution information of EV arrival times is available. Conversely, in cases where only partial distribution information of EV arrival times is known, the designed distribution-free approaches can be utilized based on the available information to solve the considered problem. Certainly, we anticipate that distribution-free approaches, which possess only partial distribution information of uncertain variables, can achieve objective values comparable to those obtained by the KSAA approach. Subsequently, we delineate the specific procedural steps of KSAA and distribution-free approaches individually.

### 4.1. K-Means Enhanced SAA Approach

The fundamental principle of stochastic programming is to characterize an uncertain set of possible realizations of the uncertain parameters. For exploring the expected total benefit, we introduce a random event set  $\Omega$ , which is indexed  $\omega$ , i.e.,  $\omega \in \Omega$  (the realization of a specific random event  $\omega \in \Omega$  can be denoted by  $\xi_\omega = \{\xi_1(\omega), \xi_2(\omega), \dots, \xi_{|\mathcal{N}|}(\omega)\}$ ) and contains infinite random events. For each random event  $\omega \in \Omega$ ,  $\xi_\omega$  is collected in the

set  $\xi = \{\xi_1, \xi_2, \dots, \xi_{|\Omega|}\}$ . Therefore, the new objective function can be reformulated as follows:

$$\min \mathbb{E}_{\xi} \left[ \sum_{j \in \mathcal{N}} \sum_{t \in \mathcal{T}} x_{jt}(\omega) \cdot c_t^e \cdot \frac{P}{60} \cdot \Delta t \right]$$

Clearly, the studied problem cannot be solved directly due to infinite random events. Thus, we adopted the SAA approach to further study the problem. In detail, we define a finite scenario set  $\mathcal{S}$ , which is indexed by  $s$ , i.e.,  $s \in \mathcal{S} = \{1, 2, \dots, |\mathcal{S}|\}$ . We formulate the realization of a specific scenario  $s \in \mathcal{S}$  as  $\zeta_s = \{\zeta_1(s), \zeta_2(s), \dots, \zeta_{|\mathcal{N}|}(s)\}$ , which is collected in the set  $\zeta = \{\zeta_1, \zeta_2, \dots, \zeta_{|\mathcal{S}|}\}$ . To make the original problem solvable, we attempt to use the finite scenario set  $\mathcal{S}$  to approximate the infinite random event set  $\Omega$ . With this assumption, the arrival time  $r_j$  for each EV  $j \in \mathcal{N}$  is known beforehand in any scenario  $s \in \mathcal{S}$ . Thus, model [P1] can be rewritten as model [P2] as shown in Appendix A. As model [P2] is a mixed-integer linear programming model, it can be readily solved by mainstream commercial solvers, such as Cplex and Gurobi.

Historically, decision-makers require a substantial set of samples  $\mathcal{S}$ , which includes a significant number of scenario samples. This extensive sampling is necessary to effectively approximate the random event set  $\Omega$  before establishing the SAA model. However, traditional SAA approaches face a limitation in terms of their computational time complexity, which exhibits a significant increasing trend with an increase in sample size  $|\mathcal{S}|$ . To overcome such a limitation, this work employs a scenario-reduction strategy inspired by Ref. [37] and utilizes the K-means method to effectively tackle the aforementioned problem. Specifically, this work initially applies the K-means method to cluster the sample set  $\mathcal{S}$  and iteratively identifies a representative set of cluster centers  $\mathcal{K} = \{1, 2, \dots, |\mathcal{K}|\}$  that is indexed by  $k$ , using Euclidean distance as a measure. Notice that the cardinality of set  $\mathcal{K}$  serves as an input parameter provided by decision-makers. The K-means approach is delineated in the following three steps, providing a comprehensive and systematic framework for data clustering:

- *Step 1:* Given the original sample set, initialize  $|\mathcal{K}|$  centers in a random manner.
- *Step 2:* Assign each scenario to the closest cluster by utilizing a classifier based on the smallest Euclidean distance.
- *Step 3:* Update the cluster centers iteratively, and repeat *Step 2* until convergence is achieved, defined as all the cluster centers remaining unchanged in the last two iterations.

Based on the K-means approach, the enhanced SAA model [P3], i.e., KSAA, can be formulated as follows:

$$[\mathbf{P3}] \min \frac{1}{|\mathcal{K}|} \cdot \sum_{k \in \mathcal{K}} \sum_{j \in \mathcal{N}} \sum_{t \in \mathcal{T}} x_{jt}(k) \cdot c_t^e \cdot \frac{P}{60} \cdot \Delta t \quad (13)$$

subject to

$$\sum_{t \in \mathcal{T}} z_{jt}(k) = 1, \quad \forall j \in \mathcal{N}, k \in \mathcal{K} \tag{14}$$

$$\sum_{j \in \mathcal{N}} x_{jt}(k) \leq \sum_{i \in \mathcal{M}} idle_{it}, \quad \forall t \in \mathcal{T}, k \in \mathcal{K} \tag{15}$$

$$x_{jt}(k) \geq z_{jt}(k), \quad \forall j \in \mathcal{N}, t \in \mathcal{T}, k \in \mathcal{K} \tag{16}$$

$$s_j(k) = \sum_{t \in \mathcal{T}} t \cdot z_{jt}(k), \quad \forall j \in \mathcal{N}, k \in \mathcal{K} \tag{17}$$

$$s_j(k) \geq r_j(k), \quad \forall j \in \mathcal{N}, k \in \mathcal{K} \tag{18}$$

$$x_{jt'}(k) \geq 1 - M \cdot (1 - z_{jt}(k)),$$

$$\forall j \in \mathcal{N}, \forall t \in \mathcal{T}, t' \in [t, t + \lceil p_j \rceil - 1], k \in \mathcal{K} \tag{19}$$

$$s_j(k) - \alpha_j(k) \cdot M \leq r_j(k) + w_{\max}, \quad \forall j \in \mathcal{N}, k \in \mathcal{K} \tag{20}$$

$$\sum_{k \in \mathcal{K}} \alpha_j(k) \leq \varepsilon \cdot |\mathcal{K}|, \quad \forall j \in \mathcal{N} \tag{21}$$

$$x_{jt}(k), z_{jt}(k), y_j(k) \in \{0, 1\}, \quad \forall j \in \mathcal{N}, t \in \mathcal{T}, k \in \mathcal{K} \tag{22}$$

$$s_j(k) \in \mathbb{R}^+, \quad \forall j \in \mathcal{N}, k \in \mathcal{K} \tag{23}$$

From the above, we can determine that both the traditional SAA method and KSAA method exhibit limitations in their ability to effectively account for the specific realization of uncertain variables that lie outside the scope of the scenario samples  $\mathcal{S}$ . In order to overcome this limitation, we now propose the adoption of distribution-free methods, which enable a tailored response to the specific realization of uncertain variables.

#### 4.2. Distribution-Free Approaches

When the probability distribution of EV arrival times is unknown but statistical bounds (e.g., upper and lower limits) are available, a distribution-free approach is adopted. This method relies on inequality-based techniques to approximate the chance constraint  $P(s_j \leq r_j + w_{\max}) \geq 1 - \varepsilon$ , ensuring robustness under partial information. By avoiding reliance on specific probability distributions, this approach is well suited for practical scenarios where only limited historical data are available.

We now primarily concentrate on addressing model **[P1]** in cases where the complete probability distribution of  $r_j$  is unknown. The statistical properties of variable  $r_j$ , including its mean, variance, as well as the upper and lower bounds, are known beforehand. In this subsection, we aim to solve the investigated problem by expanding upon the distribution-free approach proposed by Ref. [38]. In line with the distribution-free approach proposed by Ref. [38], we let

$$r_j = \bar{r}_j \cdot (1 + Z_j), \quad \forall j \in \mathcal{N} \tag{24}$$

where  $\bar{r}_j$  is the expected arrival time of EV  $j \in \mathcal{N}$ . Note that  $Z_j$  is scaled in interval  $[b_j^l, b_j^r]$ , which denotes the percentage deviation between  $r_j$  and its expected value  $\bar{r}_j$ .

It turns out that we can always find a non-positive real number  $u_j$  that can equivalently replace chance Constraint (8) with Constraint (25).

$$s_j - w_{\max} \leq \bar{r}_j + u_j, \quad \forall j \in \mathcal{N} \tag{25}$$

In contrast to Ref. [38], this work aims to approximate the chance Constraint (8) by adjusting the probability of decision variables being less than or equal to the uncertain parameter, rather than that of Ref. [38], where it is adjusted when it is not smaller than the uncertain parameter, i.e., Equation (26).

$$\mathcal{P}\{s_j - w_{\max} > r_j\} = \mathcal{P}\{s_j - w_{\max} > \bar{r}_j \cdot (1 + Z_j)\} \leq \mathcal{P}\{\bar{r}_j \cdot Z_j \leq u_j\}, \quad \forall j \in \mathcal{N} \quad (26)$$

#### 4.2.1. Case 4.2.1: Cantelli's Inequality-Based Distribution-Free Method

In this case, we assume that both  $\mathcal{P}\{Z_j < 0\}$  and  $\mathbb{E}[Z_j|Z_j < 0]$  are unknown beforehand. Due to the different expression of chance constraints compared to Ref. [38] as mentioned before, it is necessary to reformulate Equation (26) as Equation (27).

$$\mathcal{P}\{\bar{r}_j \cdot Z_j \leq u_j\} = \mathcal{P}\{-Z_j \geq -u_j/\bar{r}_j\}, \quad \forall j \in \mathcal{N} \quad (27)$$

**Theorem 1.** Equation (27) is subject to an upper bound, which can be mathematically represented as  $\frac{D(r_j)}{D(r_j)+u_j^2}$ .

**Proof.** Since the expected value of  $Z_j$  is zero, we can infer that the variance of  $Z_j$ , denoted as  $D(Z_j)$ , equals  $D(r_j)$ , divided by the square of the mean value of  $\bar{r}_j$ , i.e.,  $\mathbb{E}[Z_j^2] = D(Z_j) = \frac{D(r_j)}{\bar{r}_j^2}$ . According to Cantelli's inequality, it can be inferred that  $\mathcal{P}\{-Z_j \geq -u_j/\bar{r}_j\} \leq \frac{D(Z_j)}{D(Z_j)+(u_j/\bar{r}_j)^2} = \frac{D(r_j)}{D(r_j)+u_j^2}$ . The proof is completed.  $\square$

Given the prior knowledge of  $D(r_j)$  as mentioned before, the validity of Equation (25) can be guaranteed if an appropriate value of  $\mu_j$  that satisfies Equation (28) is identified:

$$f(\mu_j) \equiv \frac{D(r_j)}{D(r_j)+u_j^2} - \varepsilon = 0, \quad \forall j \in \mathcal{N} \quad (28)$$

The univariate root-finding algorithm in Matlab can be utilized to solve Formula (26), enabling the identification of the appropriate value for  $\mu_j$ , denoted as  $u_j^*$ .

Hence, the distribution-free model can be formulated as [P4] accordingly:

$$[\mathbf{P4}] \min \sum_{j \in \mathcal{N}} \sum_{t \in \mathcal{T}} x_{jt} \cdot c_t^e \cdot \frac{P}{60} \cdot \Delta t$$

subject to

Constraints (2)–(5), Constraint (7), Constraints (9)–(10)

$$s_j \geq \bar{r}_j \cdot (1 + b_j^r), \quad \forall j \in \mathcal{N} \quad (29)$$

$$s_j - w_{\max} \leq \bar{r}_j + u_j^*, \quad \forall j \in \mathcal{N} \quad (30)$$

#### 4.2.2. Case 4.2.2: Markov Inequality-Based Distribution-Free Method

In Case 4.2.2, we assume prior knowledge of both  $\mathcal{P}\{Z_j < 0\}$  and  $\mathbb{E}[Z_j|Z_j < 0]$ . Given that  $\mu_j \leq 0$ , it follows that  $\mathcal{P}\{\bar{r}_j \cdot Z_j \leq u_j|Z_j \geq 0\} = 0$ . Consequently, we have

$$\mathcal{P}\{\bar{r}_j \cdot Z_j \leq u_j\} = \mathcal{P}\{\bar{r}_j \cdot Z_j \leq u_j|Z_j < 0\} \cdot \mathcal{P}\{Z_j < 0\}, \quad \forall j \in \mathcal{N} \quad (31)$$

According to the Markov inequality, we have

$$\mathcal{P}\{\bar{r}_j \cdot Z_j \leq u_j\} = \mathcal{P}\{-\bar{r}_j \cdot Z_j \geq -u_j|Z_j < 0\} \cdot \mathcal{P}\{Z_j < 0\} \leq \frac{\bar{r}_j \cdot \mathbb{E}[-Z_j|Z_j < 0]}{-u_j} \cdot \mathcal{P}\{Z_j < 0\}, \quad \forall j \in \mathcal{N} \quad (32)$$

The novel distribution-free model, as illustrated in [P5], can be formulated by identifying an appropriate  $u_j$ , denoted as  $u_j^{**}$ , such that the expression  $\frac{\bar{r}_j \cdot \mathbb{E}[-Z_j | Z_j < 0]}{-u_j^{**}} \cdot \mathcal{P}\{Z_j < 0\} - \epsilon$  is equated to zero, i.e.,  $u_j^{**} = -\frac{\bar{r}_j \cdot \mathbb{E}[-Z_j | Z_j < 0] \cdot \mathcal{P}\{Z_j < 0\}}{\epsilon}$ .

$$[P5] \min \sum_{j \in \mathcal{N}} \sum_{t \in \mathcal{T}} x_{jt} \cdot c_t^e \cdot \frac{P}{60} \cdot \Delta t$$

subject to

Constraints (2)–(5), Constraint (7), Constraints (9)–(10), Constraint(29)

$$s_j - w_{\max} \leq \bar{r}_j + u_j^{**}, \quad \forall j \in \mathcal{N} \tag{33}$$

**Remark 1.** The optimal objective value of model [P4] and [P5] serves as the upper bound for that of model [P1] due to the fact that  $r_j \leq \bar{r}_j \cdot (1 + b_j)$  for each EV  $j \in \mathcal{N}$ .

#### 4.2.3. BP Neural Network-Enhanced Distribution-Free Approach

In this section, we aim to enhance the effectiveness of Cantelli’s inequality-based distribution-free approach by incorporating a BP neural network, as it demonstrates superior convergence towards the optimal value of  $u_j$  compared to the Markov inequality-based distribution-free approach when prior knowledge about the variance of EV arrival times is available.

Given the assumption of  $u_j^o$  for  $j \in \mathcal{N}$ , it can be concluded that  $\mathcal{P}\{-Z_j \geq -u_j^o / \bar{r}_j\} = \epsilon$ . Irrespective of the aforementioned version of distribution-free approaches, the upper bound obtained for  $\mathcal{P}\{-Z_j \geq -u_j / \bar{r}_j\}$  is not sufficiently tight, i.e.,  $u_j^o - u_j^* \geq 0$ . To further enhance the accuracy of this upper bound, a BP neural network algorithm is employed by this work to effectively model the gap between  $u_j^*$  and the optimal value of  $u_j$ , i.e., the maximum value of  $u_j$ . Specifically, as shown in Figure 5, we establish the connection between  $\bar{r}_j$ ,  $\sigma^2$ ,  $u_j^*$ , and  $gap_j^*$  using a BP neural network and train the BP neural network to accurately predict  $gap_j^*$  for  $j \in \mathcal{N}$ .

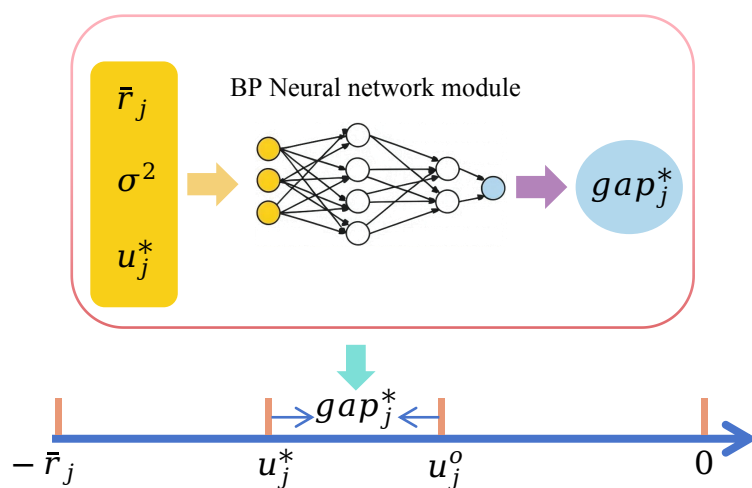


Figure 5. Illustration of the designed BP neural network-enhanced distribution-free approach.

Under the support of the BP neural network, chance Constraint (8) can be approximately replaced by Constraint (34):

$$s_j - w_{\max} \leq \bar{r}_j + u_j^* + gap_j^*, \quad \forall j \in \mathcal{N} \tag{34}$$

Certainly, considering the issue of overfitting and other factors associated with the BP neural network, it is possible for  $\mathcal{P}\{s_j \geq \bar{r}_j + u_j^* + gap_j^* + wmax\} = \varepsilon + \Delta$ , where  $\Delta > 0$ . However, when  $\Delta$  is sufficiently small, for instance,  $\Delta < 1\%$ , the  $gap_j^*$  obtained through the proposed BP neural network-enhanced distribution-free approach can be deemed acceptable.

## 5. Numerical Experiments

We utilized Matlab 2023b on a PC equipped with an i7 14700K CPU operating at 2.50 GHz and boasting 32 GB of memory to conduct numerical experiments.

Since the effectiveness of the K-means enhanced SAA approach in addressing scheduling optimization problems has been verified by both Refs. [14,37], this experiment employs the output solution of the K-means enhanced SAA approach as a benchmark to evaluate the performance of the proposed distribution-free approaches.

### 5.1. Experiment Settings

Let  $obj_{DF1a}$ ,  $obj_{DF2}$ , and  $obj_{DF1b}$ , respectively, denote the objective value of distribution-free approaches for the three versions mentioned above; the effectiveness of the three approaches is demonstrated by defining the following three relative errors:

- $gap_1 = \frac{obj_{DF1a} - obj_{KSAA}}{obj_{KSAA}} \cdot 100\%$  represents the relative error between Cantelli's inequality-based distribution-free approach and the KSAA model.
- $gap_2 = \frac{obj_{DF2} - obj_{KSAA}}{obj_{KSAA}} \cdot 100\%$  represents the relative error between the Markov inequality-based distribution-free approach and the KSAA model.
- $gap_3 = \frac{obj_{DF1b} - obj_{KSAA}}{obj_{KSAA}} \cdot 100\%$  represents the relative error between the BP neural network-enhanced distribution-free approach and the KSAA model.

The increased risk level, denoted as  $IRL$ , is defined as the difference between the actual maximum risk level obtained using the DF1b approach and the given risk level  $\epsilon$ . In other words,  $IRL$  can be calculated as  $IRL = \max_{j \in \mathcal{N}} \{\epsilon_j^{DF1b}\} - \epsilon$ , where  $\epsilon_j^{DF1b}$  represents the actual risk level obtained using DF1b. Notice that through the preliminary numerical experiments, we observed that the BP neural network comprising 8 neurons exhibited superior performance in predicting the gap between  $u_j^*$  and the optimal value of  $u_j$ . Consequently, in this numerical experiment, the number of neurons was set to 8.

We approximated the number of random events to 100,000, i.e.,  $|\Omega| = 100,000$ . The number of cluster centers  $|\mathcal{K}|$  was set as  $0.2 \cdot |\mathcal{S}|$ . In our work, the decision horizon encompasses a duration of 12 h, which is discretized into a set of time points denoted as  $\mathcal{T}$  with ten-minute intervals; thus,  $\Delta t = 10$  and  $|\mathcal{T}| = 72$ . In order to mitigate the infeasibility of the considered problem caused by randomly generated parameters, each EV charger  $i \in \mathcal{N}$  was assigned a single time period during which it would remain unavailable, accounting for only 10% to 20% of the whole decision horizon, i.e., it was scaled within the interval of  $[0.1 \cdot |\mathcal{T}|, 0.2 \cdot |\mathcal{T}|]$ . As shown in Figure 2, regarding the electricity tariffs for industrial and commercial usage in Shanghai, China, the peak and off-peak rates were established at 1.037/kWh, 0.324/kWh, and 0.648/kWh correspondingly. This work assumed that the entire decision horizon spans from 6 pm to 18 pm.

In order to comprehensively demonstrate the efficacy of the proposed approaches, we conducted numerical experiments under the assumption that the EV arrival time follows a normal distribution and a lognormal distribution, respectively. Specifically, within the normal distribution, we considered an interval of  $[10, 60]$  for a mean value of EV  $j \in \mathcal{N}$ , i.e.,  $\bar{\mu}_j$ . With reference to Ref. [39], the variance  $\bar{\sigma}^2$  was set as  $0.1 \cdot \mu_j$ . In the context of the lognormal distribution, the mean value for EV  $j \in \mathcal{N}$  was defined as  $\ln\left(\frac{\bar{\mu}_j^2}{\sqrt{\bar{\sigma}^2 + \bar{\mu}_j^2}}\right)$ ,

while the variance was specified as  $\sqrt{\ln\left(\frac{\bar{\sigma}_j^2}{\bar{\mu}_j^2} + 1\right)}$ . To enhance the feasibility of generating instances, we let  $w_{\max} = 1.2 \cdot (\max_{\omega \in \Omega}\{r_j\} - (\bar{r}_j + \mu_j^*))$  under the two distributions. The other parameter settings are presented in Table 2.

**Table 2.** Parameter settings.

Parameters:	$ S $	$l_j$	$v_1$	$v_2$	$\varepsilon$	$P$
Values:	100	[80, 100]	1	0.5	0.1	60

## 5.2. Numerical Results

The numerical results presented in Tables A1 and A2 in Appendix B were used to compare the performance of KSAA against the three proposed distribution-free approaches (DF1a, DF2, and DF1b) under both normal and lognormal distributions. The comparison was conducted with varying scaling intervals for parameter  $a_j$ : [20, 60] in Table A1 and [20, 30] in Table A2. The findings highlight the significant advantages of the distribution-free approaches in terms of both computational efficiency and solution accuracy.

The average running times of KSAA are substantially higher compared to the proposed methods. Specifically, for the [20, 60] interval, the average computational times of KSAA, DF1a, DF2, and DF1b are 2623, 18, 18, and 20 s, respectively, as shown in Table A1. Similarly, under the [20, 30] interval (Table A2), the average running times are 2549, 19, 19, and 20 s. These results correspond to a reduction in execution time of approximately 99.31%, 99.31%, and 99.24% for DF1a, DF2, and DF1b compared to KSAA under the [20, 60] interval, and 99.25%, 99.25%, and 99.22% under the [20, 30] interval. Notably, DF1b exhibits a slightly longer running time (by approximately 2 s) than DF1a and DF2, a trade-off that is compensated by its superior accuracy.

Regardless of the method, the computational time shows a noticeable upward trend with an increasing number of EVs, while the number of EV chargers has only a negligible impact on running time. This scalability further underscores the practicality of the proposed methods for real-world applications.

The relative errors of the proposed methods vary depending on the approach and the underlying distribution. Under the [20, 60] interval, the average relative errors for DF1a, DF2, and DF1b are 5.15%, 7.21%, and 2.09%, respectively, with DF1b consistently achieving the smallest error. Under the [20, 30] interval, the corresponding relative errors are 4.78%, 7.08%, and 2.03%, again demonstrating the superior accuracy of DF1b. These results suggest that DF1b can effectively predict objective values and generate feasible scheduling solutions, even with limited information about the uncertain variable  $r_j$ .

Figure 6 provides a detailed visualization of the relative errors ( $gap_1$ ,  $gap_2$ , and  $gap_3$ ) for instances 1 to 48 (Table A1 presents the  $gap$  values of the solutions obtained by each method for instances 1 to 24, while Table A2 shows the  $gap$  values for the remaining instances) across the three distribution-free approaches. The bar chart highlights the differences in prediction accuracy among the methods. DF1b ( $gap_3$ , green bars) consistently achieves the smallest relative error across all instances, with most values below 6%. By contrast, DF2 ( $gap_2$ , orange bars) often exhibits the largest errors, with many values exceeding 10%. DF1a ( $gap_1$ , blue bars) demonstrates intermediate performance, with errors generally higher than DF1b but lower than DF2. This visual evidence aligns with the numerical results, reinforcing the conclusion that DF1b is the most accurate and robust approach. Figure 6 also emphasizes the stability of DF1b, as its error distribution remains tightly bounded compared to the larger variance observed in DF2.

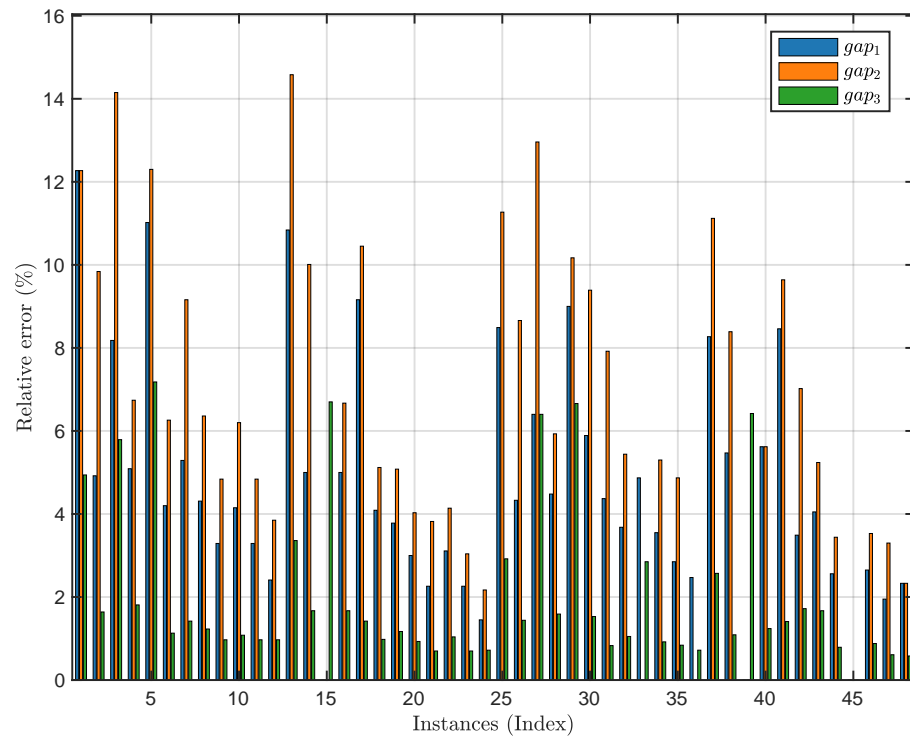


**Figure 6.** Comparison of relative error distributions.

The performance of the proposed approaches is influenced by the type of distribution. DF1b demonstrates higher relative accuracy under lognormal distributions compared to normal distributions. This can be attributed to the concentration of EV arrival times near the mean under lognormal distributions, which enhances the fitting capability of the BP neural network used in this study. By contrast, DF2's accuracy is hindered by its limited capacity to incorporate variance information, resulting in the highest relative errors among the three distribution-free approaches.

In terms of integrated risk level (*IRL*), DF1b achieves an average increase of less than 0.30% across all settings, effectively balancing robustness and feasibility. It successfully mitigates the conservatism inherent in traditional distribution-free methods and addresses the infeasibility and time constraints associated with KSAA. Notably, DF1b overcomes the inability of KSAA to generate feasible solutions for certain instances (as indicated by missing values in Tables A1 and A2).

Overall, numerical experiments demonstrate the effectiveness of both the SAA and distribution-free approaches in handling the uncertainty of EV arrival times. Under known probability distributions, the SAA method provides robust and cost-effective schedules by leveraging scenario generation. In contrast, the distribution-free approach shows strong performance in cases where only partial information (e.g., upper and lower bounds) is available, ensuring reliable scheduling decisions without relying on specific distributional assumptions.

In terms of managerial insights, the aforementioned conclusion suggests the following. (1) The inherent uncertainty in EV arrival times necessitates robust scheduling strategies. SAA enables the creation of schedules that perform well on average across multiple scenarios, while distribution-free approaches provide solutions that are resilient to a wide range of possible arrival time distributions. Managers should consider integrating these approaches to enhance the reliability of charging station operations. (2) Distribution-free approaches offer scalability and adaptability to varying levels of demand and uncertainty, making them versatile tools for diverse operating environments. Managers can leverage these techniques to scale operations efficiently and adapt to dynamic changes in EV usage

patterns. (3) By optimizing charging schedules with these advanced methods, it is possible to reduce operational costs. Efficient scheduling minimizes peak load, reduces the need for expensive infrastructure upgrades, and optimizes energy usage. This cost-effectiveness is crucial for maintaining competitive pricing and ensuring the financial sustainability of EV charging services. And (4) the integration of these approaches encourages a data-driven approach to decision-making. By continuously collecting and analyzing data on EV arrivals and charging patterns, managers can refine their scheduling algorithms and improve performance over time.

## 6. Conclusions

In this work, we study an EV charging scheduling problem, where the arrival time of each EV is uncertain. A K-means enhanced SAA together with two versions of distribution-free approaches are proposed to solve this problem. Additionally, a BP neural network is also applied to enhance the proposed distribution-free approach.

Numerical experiments demonstrate the effectiveness of the model in reducing total charging costs while ensuring the reliability of scheduling decisions under diverse uncertainty conditions. The results highlight that the proposed methods can adapt to different levels of uncertainty and provide practical solutions for EV charging stations, even under challenging real-world conditions. The results show that balancing robustness and cost efficiency is essential for designing effective charging schedules, and the proposed methods achieve this balance through tailored optimization techniques. Additionally, numerical results confirm the computational feasibility of the model for small-to-medium problem sizes, demonstrating its applicability to real-world EV charging stations.

The assumptions of uninterrupted charging and fixed TOU pricing simplify the model for mathematical tractability but may limit its applicability in real-world scenarios. Charging interruptions, caused by user behavior or operational constraints, could significantly impact the scheduling process but are not currently accounted for in this study. Similarly, fixed TOU pricing does not reflect real-time pricing dynamics or demand response programs, which are increasingly common in modern power systems. Future research directions may include the following: (1) exploring more effective clustering approaches to enhance the traditional stochastic programming approaches; (2) extending the model to accommodate real-time or dynamic pricing schemes, such as demand response programs, to capture the variability in electricity prices and their impact on scheduling decisions; (3) developing other deep learning enhanced methods which require less training time of large-scale data; (4) conducting a formal sensitivity analysis to evaluate the impact of key parameter variations, such as charging rates, arrival times, and cost structures, on the model's outcomes; and (5) testing the scalability of the proposed approach on larger datasets and in more complex scenarios, such as highly variable EV arrival patterns or larger fleets, using advanced optimization techniques or real-time dynamic scheduling frameworks to ensure robustness and practicality in real-world applications.

**Author Contributions:** Conceptualization, Z.W. and F.Z.; methodology, M.L.; software, Z.W.; validation, F.Z., and M.L.; formal analysis, Z.W.; investigation, Z.W.; resources, Z.W.; writing—original draft preparation, Z.W.; writing—review and editing, F.Z.; supervision, F.Z., and M.L. All authors have read and agreed to the published version of the manuscript.

**Funding:** This work was partially supported by the National Natural Science Foundation of China (Grant Nos. 72271051, 71832001, 72021002 and 72071144) and the Fundamental Research Funds for the Central Universities (Grant No. 2232018 H-07).

**Institutional Review Board Statement:** Not applicable.

**Informed Consent Statement:** Not applicable.

**Data Availability Statement:** The data supporting the findings of this study are available from the corresponding author upon reasonable request.

**Conflicts of Interest:** The authors declare no conflicts of interest.

## Appendix A. The SAA Model

We first introduce a binary auxiliary variable  $\alpha_j(s)$  ( $j \in \mathcal{N}, j \in \mathcal{N}$ ), and then present the SAA model:

$\alpha_j(s)$ : A binary auxiliary variable, when equal to 1 indicates that  $s_j(s) > r_j(s) + w_{\max}$ , or 0 otherwise.

Under the support of the scenario set  $\mathcal{S}$ , the SAA model can be formulated as follows:

$$[\mathbf{P2}] \min \frac{1}{|\mathcal{S}|} \cdot \sum_{s \in \mathcal{S}} \sum_{j \in \mathcal{N}} \sum_{t \in \mathcal{T}} x_{jt}(s) \cdot c_t^e \cdot \frac{P}{60} \cdot \Delta t \quad (\text{A1})$$

subject to

$$\sum_{t \in \mathcal{T}} z_{jt}(s) = 1, \quad \forall j \in \mathcal{N}, \forall s \in \mathcal{S} \quad (\text{A2})$$

$$\sum_{j \in \mathcal{N}} x_{jt}(s) \leq \sum_{i \in \mathcal{M}} \text{idle}_{it}, \quad \forall t \in \mathcal{T}, \forall s \in \mathcal{S} \quad (\text{A3})$$

$$x_{jt}(s) \geq z_{jt}(s), \quad \forall j \in \mathcal{N}, t \in \mathcal{T}, s \in \mathcal{S} \quad (\text{A4})$$

$$s_j(s) = \sum_{t \in \mathcal{T}} t \cdot z_{jt}(s), \quad \forall j \in \mathcal{N}, \forall s \in \mathcal{S} \quad (\text{A5})$$

$$s_j(s) \geq r_j(s), \quad \forall j \in \mathcal{N}, \forall s \in \mathcal{S} \quad (\text{A6})$$

$$x_{jt'}(s) \geq 1 - M \cdot (1 - z_{jt}(s)),$$

$$\forall j \in \mathcal{N}, \forall t \in \mathcal{T}, \forall t' \in [t, t + [p_j] - 1], \forall s \in \mathcal{S} \quad (\text{A7})$$

$$s_j(s) - \alpha_j(s) \cdot M \leq r_j(s) + w_{\max}, \quad \forall j \in \mathcal{N}, \forall s \in \mathcal{S} \quad (\text{A8})$$

$$\sum_{s \in \mathcal{S}} \alpha_j(s) \leq \varepsilon \cdot |\mathcal{S}|, \quad \forall j \in \mathcal{N} \quad (\text{A9})$$

$$x_{jt}(s), z_{jt}(s), y_j(s) \in \{0, 1\}, \quad \forall j \in \mathcal{N}, \forall t \in \mathcal{T}, \forall s \in \mathcal{S} \quad (\text{A10})$$

$$s_j(s) \in \mathbb{R}^+, \quad \forall j \in \mathcal{N}, \forall s \in \mathcal{S} \quad (\text{A11})$$

Constraint (A2) ensures that each EV  $j \in \mathcal{N}$  must be charged in each scenario  $s \in \mathcal{S}$  throughout the entire time horizon. Constraint (A3) guarantees that the number of EVs charged at any time  $t \in \mathcal{T}$  is not larger than that of the given EV chargers for each scenario  $s \in \mathcal{S}$ . Constraints (A4)–(A6) calculate the start charging time of EV  $j \in \mathcal{N}$  for each scenario  $s \in \mathcal{S}$ . Constraint (A7) guarantees that the charging duration of EV  $j \in \mathcal{N}$  is continuous and uninterrupted for each scenario  $s \in \mathcal{S}$ . Constraints (A8)–(A9) guarantee that the probability of the start charging time being greater than  $r_j + w_{\max}$  cannot be greater than the given risk level  $\varepsilon$  under the scenario set  $\mathcal{S}$ . Constraints (A10)–(A11) give the range of variables.

## Appendix B. Numerical Results

This section presents the results of two numerical experiments conducted to evaluate the performance of the proposed approach. The results are summarized in Tables A1 and A2, which highlight key metrics and trends observed during the experiments.

**Table A1.** Numerical results for the case where  $a_j$  is scaled in interval  $[20, 60]$ .

Instances ( $\mathcal{M}, \mathcal{N}$ )	KSAA		DF1a			DF2			DF1b			IRL (%)
	$obj_{KSAA}$	time(s)	$obj_{DF1a}$	time(s)	$gap_1(\%)$	$obj_{DF2}$	time(s)	$gap_2(\%)$	$obj_{DF1b}$	time(s)	$gap_3(\%)$	
Normal distribution												
(2,3)	106.21	243	119.24	4	12.27	119.24	4	12.27	111.46	9	4.94	0.13
(2,5)	237.17	617	248.84	7	4.92	260.51	7	9.84	241.06	8	1.64	0.00
(2,7)	325.89	1559	352.54	12	8.18	371.99	12	14.15	344.76	14	5.79	0.47
(3,5)	236.78	742	248.84	8	5.09	252.73	8	6.74	241.06	10	1.81	0.00
(3,7)	303.53	1523	336.98	13	11.02	340.87	13	12.30	325.31	15	7.18	0.47
(3,9)	379.34	3257	395.29	18	4.20	403.07	18	6.26	383.62	20	1.13	0.30
(4,7)	301.58	2739	317.53	13	5.29	329.20	13	9.16	305.86	15	1.42	0.47
(4,9)	378.95	2382	395.29	20	4.31	403.07	20	6.36	383.62	21	1.23	0.30
(4,11)	501.87	3389	518.41	21	3.29	526.19	21	4.84	506.74	23	0.97	0.10
(5,9)	379.54	4363	395.29	18	4.15	403.07	18	6.20	383.62	26	1.08	0.30
(5,11)	501.88	2991	518.41	19	3.29	526.19	19	4.84	506.74	21	0.97	0.10
(5,13)	540.37	7159	553.40	21	2.41	561.18	21	3.85	545.62	23	0.97	0.51
Lognormal distribution												
(2,3)	104.07	326	115.35	4	10.84	119.24	4	14.58	107.57	6	3.36	0.13
(2,5)	233.28	620	244.95	6	5.00	256.62	6	10.01	237.17	18	1.67	0.00
(2,7)	319.48	1562	-	12	-	-	12	-	340.87	12	6.70	0.50
(3,5)	233.28	670	244.95	8	5.00	248.84	8	6.67	237.17	9	1.67	0.00
(3,7)	301.58	1546	329.20	13	9.16	333.09	13	10.45	305.86	14	1.42	0.50
(3,9)	376.03	2399	391.40	18	4.09	395.29	18	5.12	379.73	20	0.98	0.30
(4,7)	298.47	1536	309.75	13	3.78	313.64	13	5.08	301.97	15	1.17	0.50
(4,9)	376.23	2786	387.51	19	3.00	391.40	19	4.03	379.73	21	0.93	0.30
(4,11)	499.35	3666	510.63	22	2.26	518.41	21	3.82	502.85	24	0.70	0.11
(5,9)	375.84	2876	387.51	17	3.11	391.40	17	4.14	379.73	19	1.04	0.30
(5,11)	499.35	6589	510.63	20	2.26	514.52	20	3.04	502.85	22	0.70	0.11
(5,13)	537.84	7421	545.62	104	1.45	549.51	106	2.17	541.73	101	0.72	0.57
Average	347.83	2623	364.24	18	5.15	370.83	18	7.21	354.03	20	2.09	0.27

Note: “-” indicates that the generated instance is not feasible for the model.

**Table A2.** Numerical results for the case where  $a_j$  is scaled in interval [20, 30].

Instances ( $\mathcal{M}, \mathcal{N}$ )	KSAA		DF1a			DF2			DF1b			IRL (%)
	$obj_{KSAA}$	time(s)	$obj_{DF1a}$	time(s)	$gap_1(\%)$	$obj_{DF2}$	time(s)	$gap_2(\%)$	$obj_{DF1b}$	time(s)	$gap_3(\%)$	
Normal distribution												
(2,3)	139.78	256	151.64	4	8.49	155.53	4	11.27	143.86	6	2.92	0.13
(2,5)	269.57	1547	281.24	9	4.33	292.91	7	8.66	273.46	9	1.44	0.00
(2,7)	355.70	1390	378.46	12	6.40	401.80	12	12.96	378.46	13	6.40	0.47
(3,5)	269.18	678	281.24	7	4.48	285.13	7	5.93	273.46	9	1.59	0.00
(3,7)	332.95	1403	362.90	13	9.00	366.79	13	10.17	355.12	14	6.66	0.47
(3,9)	445.50	3661	471.76	16	5.89	487.32	16	9.39	452.31	18	1.53	0.30
(4,7)	329.06	1168	343.45	10	4.37	355.12	10	7.92	331.78	20	0.83	0.47
(4,9)	443.75	3494	460.09	108	3.68	467.87	105	5.44	448.42	79	1.05	0.30
(4,11)	579.64	4394	607.84	25	4.87	-	24	-	596.17	24	2.85	0.10
(5,9)	444.34	2609	460.09	19	3.55	467.87	19	5.30	448.42	23	0.92	0.30
(5,11)	579.64	4028	596.17	27	2.85	607.84	27	4.87	584.50	29	0.84	0.10
(5,13)	670.36	5808	686.89	28	2.47	-	28	-	675.22	28	0.72	0.51
Lognormal distribution												
(2,3)	136.47	287	147.75	4	8.27	151.64	4	11.12	139.97	5	2.57	0.13
(2,5)	266.65	726	281.24	7	5.47	289.02	8	8.39	269.57	9	1.09	0.00
(2,7)	348.31	1402	-	12	-	-	12	-	370.68	12	6.42	0.50
(3,5)	266.26	773	281.24	8	5.62	281.24	8	5.62	269.57	9	1.24	0.00
(3,7)	331.00	1765	359.01	13	8.46	362.90	13	9.64	335.67	15	1.41	0.50
(3,9)	440.83	3371	456.20	18	3.49	471.76	18	7.02	448.42	20	1.72	0.30
(4,7)	326.33	1788	339.56	13	4.05	343.45	13	5.24	331.78	15	1.67	0.50
(4,9)	441.03	2601	452.31	19	2.56	456.20	19	3.44	444.53	23	0.79	0.30
(4,11)	577.10	2992	-	17	-	-	17	-	-	16	-	0.11
(5,9)	440.64	2760	452.31	19	2.65	456.20	19	3.53	444.53	21	0.88	0.30
(5,11)	577.11	3809	588.39	25	1.95	596.17	25	3.30	580.61	27	0.61	0.11
(5,13)	667.44	8469	683.00	26	2.33	683.00	25	2.33	671.33	27	0.58	0.57
Average	403.28	2549	414.67	19	4.78	398.99	19	7.08	402.95	20	2.03	0.27

Note: “-” indicates that the generated instance is not feasible for the model.

## References

1. Roy, S.; Lam, Y.F.; Hung, N.T.; Chan, J.C.L. Development of on-road emission inventory and evaluation of policy intervention on future emission reduction toward sustainability in Vietnam. *Sustain. Dev.* **2021**, *29*, 1072–1085.
2. Park, K.; Moon, I. Multi-agent deep reinforcement learning approach for EV charging scheduling in a smart grid. *Appl. Energy* **2022**, *328*, 120111.
3. Yin, W.J.; Qin, X. Cooperative optimization strategy for large-scale electric vehicle charging and discharging. *Energy* **2022**, *258*, 124969.
4. Shahmoradi, H.; Esmaelian, M.; Karshenas, H. An EDA-based method for solving electric vehicle charging scheduling problem under limited power and maximum imbalance constraints. *Comput. Ind. Eng.* **2022**, *172*, 108544.
5. Huang, Q.L.; Yang, L.; Hou, C.; Zeng, Z.Y.; Qi, Y.W. Event-based EV charging scheduling in a microgrid of buildings. *IEEE Trans. Transp. Electrification* **2023**, *9*, 1784–1796.
6. Shao, S.P.; Sartipizadeh, H.; Gupta, A. Scheduling EV charging having demand with different reliability constraints. *IEEE Trans. Intell. Transp. Syst.* **2023**, *24*, 11018–11029.
7. Lampon, J.F. Efficiency in design and production to achieve sustainable development challenges in the automobile industry: Modular electric vehicle platforms. *Sustain. Dev.* **2023**, *31*, 26–38.
8. Ullah, Z.; Wang, S.R.; Wu, G.; Hasanien, H.M.; Rehman, A.U.; Turkey, R.A.; Elkadeem, M.R. Optimal scheduling and techno-economic analysis of electric vehicles by implementing solar-based grid-tied charging station. *Energy* **2023**, *267*, 126560.
9. Wu, J.; Su, H.; Meng, J.H.; Lin, M.Q. Electric vehicle charging scheduling considering infrastructure constraints. *Energy* **2023**, *278*, 127806.
10. de Sa, A.L.S.; Lavieri, P.S.; Cheng, Y.T.; Hajhashemi, E.; Oliveira, G.J.M. Modelling driver's response to demand management strategies for electric vehicle charging in Australia. *Energy Res. Soc. Sci.* **2023**, *103*, 103218.
11. Montoya, A.; Gueret, C.; Mendoza, J.E.; Villegas, J.G. The electric vehicle routing problem with nonlinear charging function. *Transp. Res. Part B* **2017**, *103*, 87–110.
12. Xu, M.; Meng, Q. Fleet sizing for one-way electric carsharing services considering dynamic vehicle relocation and nonlinear charging profile. *Transp. Res. Part B* **2019**, *128*, 23–49.
13. Zhang, L.; Wang, S.; Qu, X. Optimal electric bus fleet scheduling considering battery degradation and non-linear charging profile. *Transp. Res. Part E* **2021**, *154*, 102445.
14. Zheng, F.F.; Wang, Z.J.; Liu, M. Charging scheduling of battery electric buses with uncertain charging time. *Oper. Res.* **2022**, *22*, 4865–4903.
15. Luo, Y.G.; Feng, G.X.; Wan, S.; Zhang, S.W.; Li, V.; Kong, W.W. Charging scheduling strategy for different electric vehicles with optimization for convenience of drivers, performance of transport system and distribution network. *Energy* **2020**, *194*, 116807.
16. Wu, F.Z.; Yang, J.; Zhan, X.P.; Liao, S.Y.; Xu, J. The online charging and discharging scheduling potential of electric vehicles considering the uncertain responses of users. *IEEE Trans. Power Syst.* **2021**, *36*, 1794–1806.
17. Xie, D.F.; Yu, Y.P.; Zhou, G.J.; Zhao, X.M.; Chen, Y.J. Collaborative optimization of electric bus line scheduling with multiple charging modes. *Transp. Res. Part D* **2023**, *114*, 103551.
18. Sassi, O.; Oulamara, A. Electric vehicle scheduling and optimal charging problem: Complexity, exact and heuristic approaches. *Int. J. Prod. Res.* **2017**, *55*, 519–535.
19. Koufakis, A.M.; Rigas, E.S.; Bassiliades, N.; Ramchurn, S.D. Offline and online electric vehicle charging scheduling with V2V energy transfer. *IEEE Trans. Intell. Transp. Syst.* **2020**, *21*, 2128–2138.
20. Kakkar, R.; Gupta, R.; Agrawal, S.; Tanwar, S.; Altameem, A.; Altameem, T.; Sharma, R.; Turcanu, F.E.; Raboaca, M.S. Blockchain and IoT-driven optimized consensus mechanism for electric vehicle scheduling at charging stations. *Sustainability* **2022**, *14*, 12800.
21. Cao, Y.S.; Wang, Y.Q.; Li, D.M.; Chen, X.M. Joint routing and wireless charging scheduling for electric vehicles with shuttle services. *IEEE Internet Things J.* **2023**, *10*, 14810–14819.
22. Wang, W.L.; Wu, L. A semi-decentralized real-time charging scheduling scheme for large EV parking lots considering uncertain EV arrival and departure. *IEEE Trans. Smart Grid* **2024**, *15*, 5871–5884.
23. Hossain, M.B.; Pokhrel, S.R.; Vu, H.L. Efficient and private scheduling of wireless electric vehicles charging using reinforcement learning. *IEEE Trans. Intell. Transp. Syst.* **2023**, *24*, 4089–4102.
24. Wang, H.; Shi, M.G.; Xie, P.; Lai, C.S.; Jia, Y.W. Electric vehicle charging scheduling strategy for supporting load flattening under uncertain electric vehicle departures. *J. Mod. Power Syst. Clean Energy* **2023**, *11*, 1634–1645.
25. Nimalsiri, N.I.; Ratnam, E.L.; Smith, D.B.; Mediwaththe, C.P.; Halgamuge, S.K. Coordinated charge and discharge scheduling of electric vehicles for load curve shaping. *IEEE Trans. Intell. Transp. Syst.* **2022**, *23*, 7653–7665.
26. Frendo, O.; Gaertner, N.; Stuckenschmidt, H. Open source algorithm for smart charging of electric vehicle fleets. *IEEE Trans. Ind. Inform.* **2021**, *17*, 6014–6022.
27. Zhao, Z.H.; Lee, C.K.M.; Ren, J.Z. A two-level charging scheduling method for public electric vehicle charging stations considering heterogeneous demand and nonlinear charging profile. *Appl. Energy* **2024**, *355*, 122278.

28. Aljohani, T.; Mohamed, M.A.; Mohammed, O. Tri-level hierarchical coordinated control of large-scale EVs charging based on multi-layer optimization framework. *Electr. Power Syst. Res.* **2024**, *226*, 109923.
29. Jia, Y.; Wang, Y.; Bai, H.; Wang, S.; Li, Q.; Hua, Y. Electric vehicles participate in the economic optimal scheduling method of virtual power plant considering time-of-use tariff. In Proceedings of the 2023 IEEE Power Electronics and Power Systems Conference (PEPSC), Chongqing, China, 24–26 November 2023; pp. 267–275. <https://doi.org/10.1109/PEPSC58749.2023.10394837>.
30. Tan, M.; Ren, Y.L.; Pan, R.; Wang, L.; Chen, J. Fair and efficient electric vehicle charging scheduling optimization considering the maximum individual waiting time and operating cost. *IEEE Trans. Veh. Technol.* **2023**, *72*, 9808–9820.
31. Arikumar, K.S.; Prathiba, S.B.; Moorthy, R.S.; Srivastava, G.; Gadekallu, T.R. Software defined networking assisted electric vehicle charging: Towards smart charge scheduling and management. *IEEE Trans. Netw. Sci. Eng.* **2024**, *11*, 163–173.
32. de Vos, M.H.; van Lieshout, R.N.; Dollevoet, T. Electric vehicle scheduling in public transit with capacitated charging stations. *Transp. Sci.* **2024**, *58*, 279–294.
33. Chen, J.; Huang, X.Q.; Cao, Y.J.; Li, L.Y.; Yan, K.; Wu, L.; Liang, K. Electric vehicle charging schedule considering shared charging pile based on Generalized Nash Game. *Int. J. Electr. Power Energy Syst.* **2022**, *136*, 107579.
34. Diefenbach, H.; Emde, S.; Glock, C.H. Multi-depot electric vehicle scheduling in in-plant production logistics considering non-linear charging models. *Eur. J. Oper. Res.* **2023**, *306*, 828–848.
35. Zhou, S.; Zhang, D.; Ji, B.; Zhou, S.; Li, S.; Zhou, L. A MILP model and heuristic method for the time-dependent electric vehicle routing and scheduling problem with time windows. *J. Clean. Prod.* **2024**, *434*, 140188.
36. Ke, B.; Chung, Y.C.; Chen, Y.C. Minimizing the costs of constructing an all plug-in electric bus transportation system: A case study in Penghu. *Appl. Energy* **2016**, *177*, 649–660.
37. Emelogu, A.; Chowdhury, S.; Marufuzzaman, M.; Bian, L.; Eksioglu, B. An enhanced sample average approximation method for stochastic optimization. *Int. J. Prod. Econ.* **2016**, *182*, 230–252.
38. Ng, M. Distribution-free vessel deployment for liner shipping. *Eur. J. Oper. Res.* **2014**, *238*, 858–862.
39. Liu, X.; Chu, F.; Zheng, F.F.; Chu, C.B.; Liu, M. Parallel machine scheduling with stochastic release times and processing times. *Int. J. Prod. Res.* **2021**, *59*, 6327–6346.

**Disclaimer/Publisher’s Note:** The statements, opinions and data contained in all publications are solely those of the individual author(s) and contributor(s) and not of MDPI and/or the editor(s). MDPI and/or the editor(s) disclaim responsibility for any injury to people or property resulting from any ideas, methods, instructions or products referred to in the content.